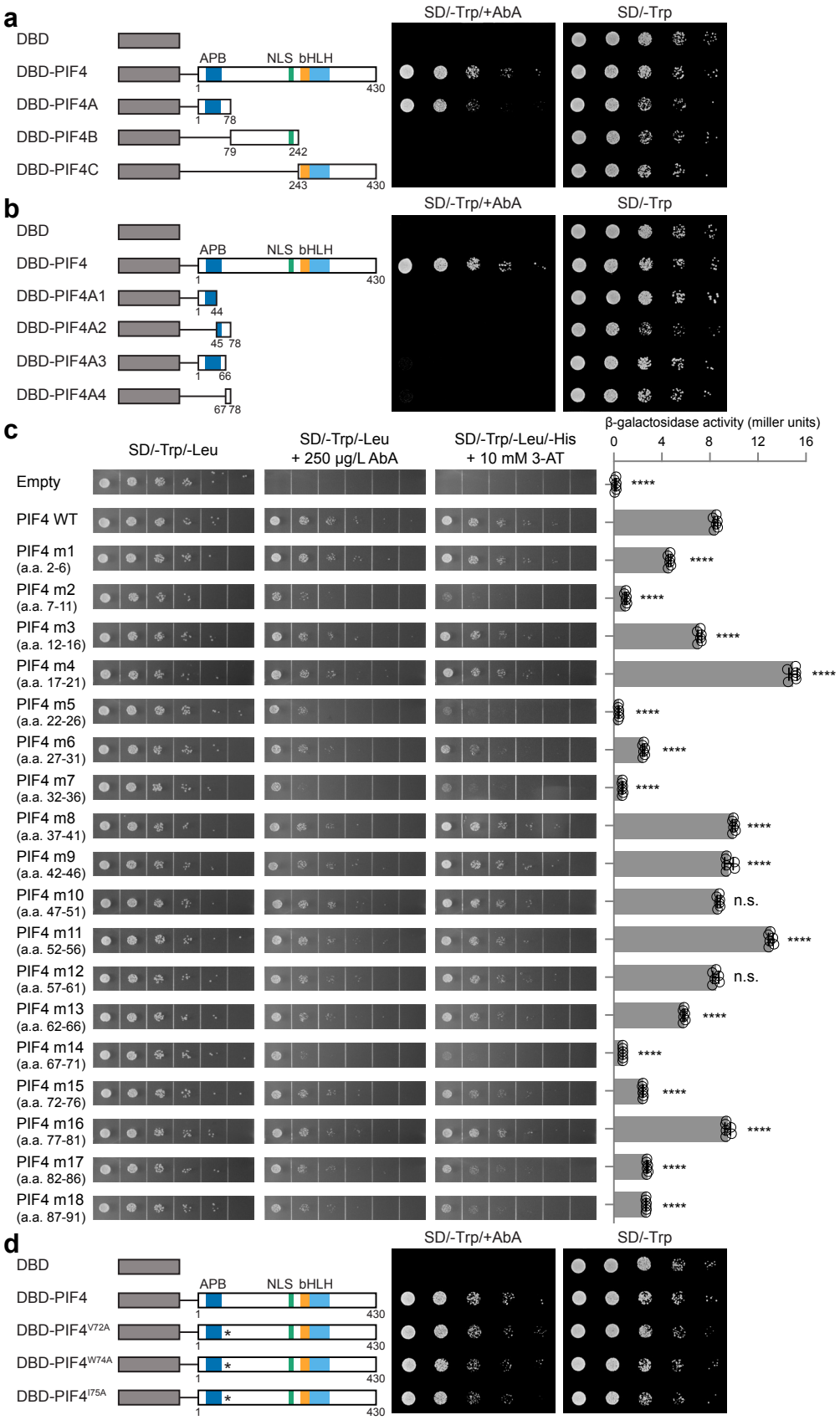

Supplementary Figure 1. Identification of the residues necessary for PIF4's TAD activity via alanine-scanning mutagenesis. a, The N-terminal 78 amino acids of PIF4 confer strong transactivation activity in yeast. **b**, Further fragmentations of the N-terminal 78 amino acids completely abolish the transactivation activity in yeast. **c**, Three yeast reporters, Aureobasidin A (AbA) resistance, HIS3 (-His), and LacZ (β-galactosidase liquid assay), are used to determine the activity of PIF4 wild-type and mutant versions. **d**, Mutating individual hydrophobic residues in M15 does not affect the transactivation activity of PIF4 in yeast.

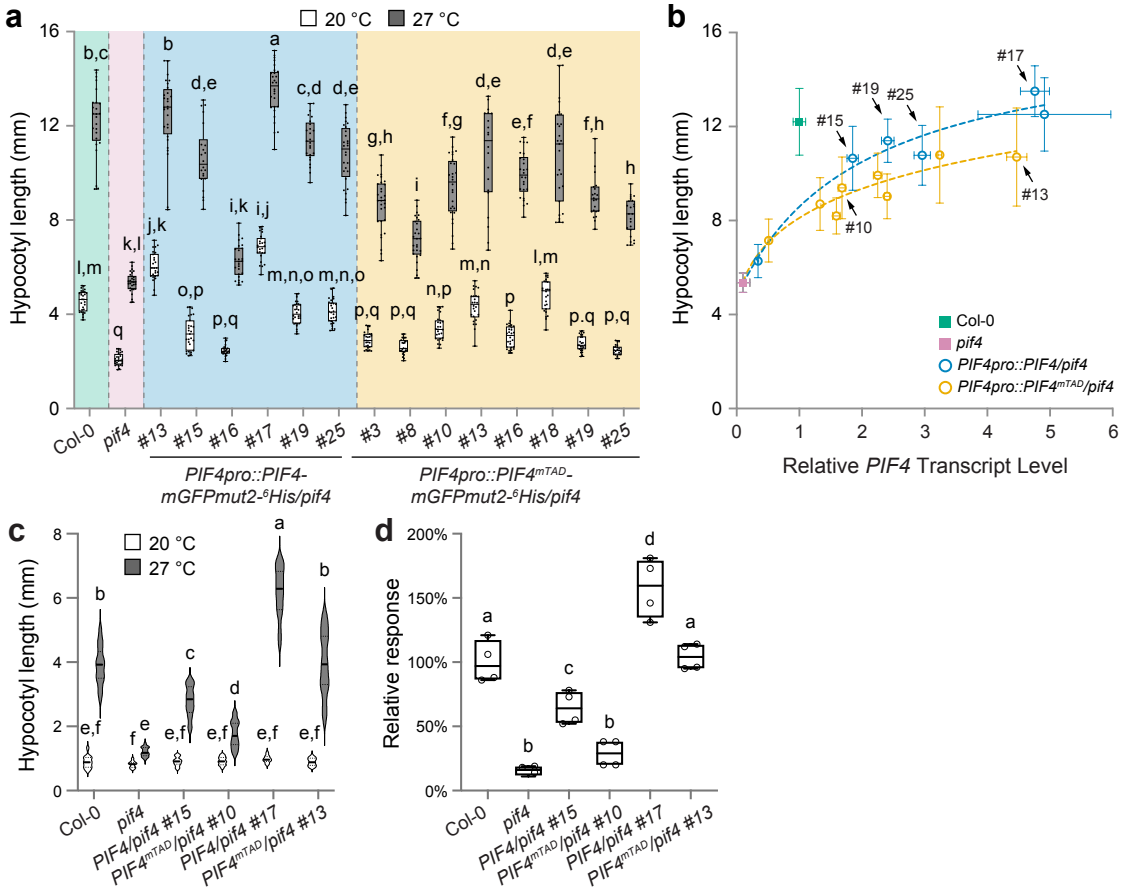

Supplementary Figure 2. Characterizations of *PIF4* transgenic lines in the *pif4* mutant background. a, Hypocotyl length measurements of seedlings. Wild-type (Col-0), *pif4-2* mutant, and transgenic lines expressing *PIF4-mGFPmut2-^{6}His* or *PIF4^{mTAD}-mGFPmut2-^{6}His* driven by the *PIF4* native promoter in the *pif4-2* mutant background were grown for 5 days in continuous red (Rc) light (50 μmol m^{-2} s^{-1}). The white and grey boxes represent hypocotyl length at 20 °C and 27 °C, respectively. The elements of box plots are as follows: center line, median; box limits, first and third quartiles; whiskers, minimum and maximum values; points, all data points. **b**, Relationship between *PIF4* transcript level and hypocotyl length at warm temperatures. The hypocotyl length of each genotype grown at 27 °C in **a** was plotted against the relative *PIF4* transcript level measured in the same condition (that in Col-0 was set to 1). Nonlinear regression (sigmoidal, 4PL) was performed separately for *PIF4-mGFPmut2-^{6}His/pif4* (blue) and *PIF4^{mTAD}-mGFPmut2-^{6}His/pif4* lines (yellow). Arrows and numbers indicate the transgenic lines selected for further studies. **c**, Hypocotyl length measurements of seedlings grown for 4 days in white light (16-h light/8-h night, 125 μmol m^{-2} s^{-1}). The white and grey violin plots represent hypocotyl length measurements at 20 °C and 27 °C, respectively. The elements of violin plots are as follows: solid line, median; lower dotted line, first quartile; upper dotted line, third quartile. Different letters denote significant statistical differences between the absolute hypocotyl length of each line (two-way ANOVA, n ≥ 38, $p < 0.01$). **d**, Comparison of the relative thermal response among the seedlings. The elements of box plots are as follows: center line, median; box limits, first and third quartiles; whiskers, minimum and maximum values; points, all data points. The relative response is defined as the relative hypocotyl response to 27 °C of a mutant compared with that of Col-0 (which is set at 100%). Different letters denote significant statistical differences between the relative response of each genotype (one-way ANOVA, n = 4, $p < 0.05$).

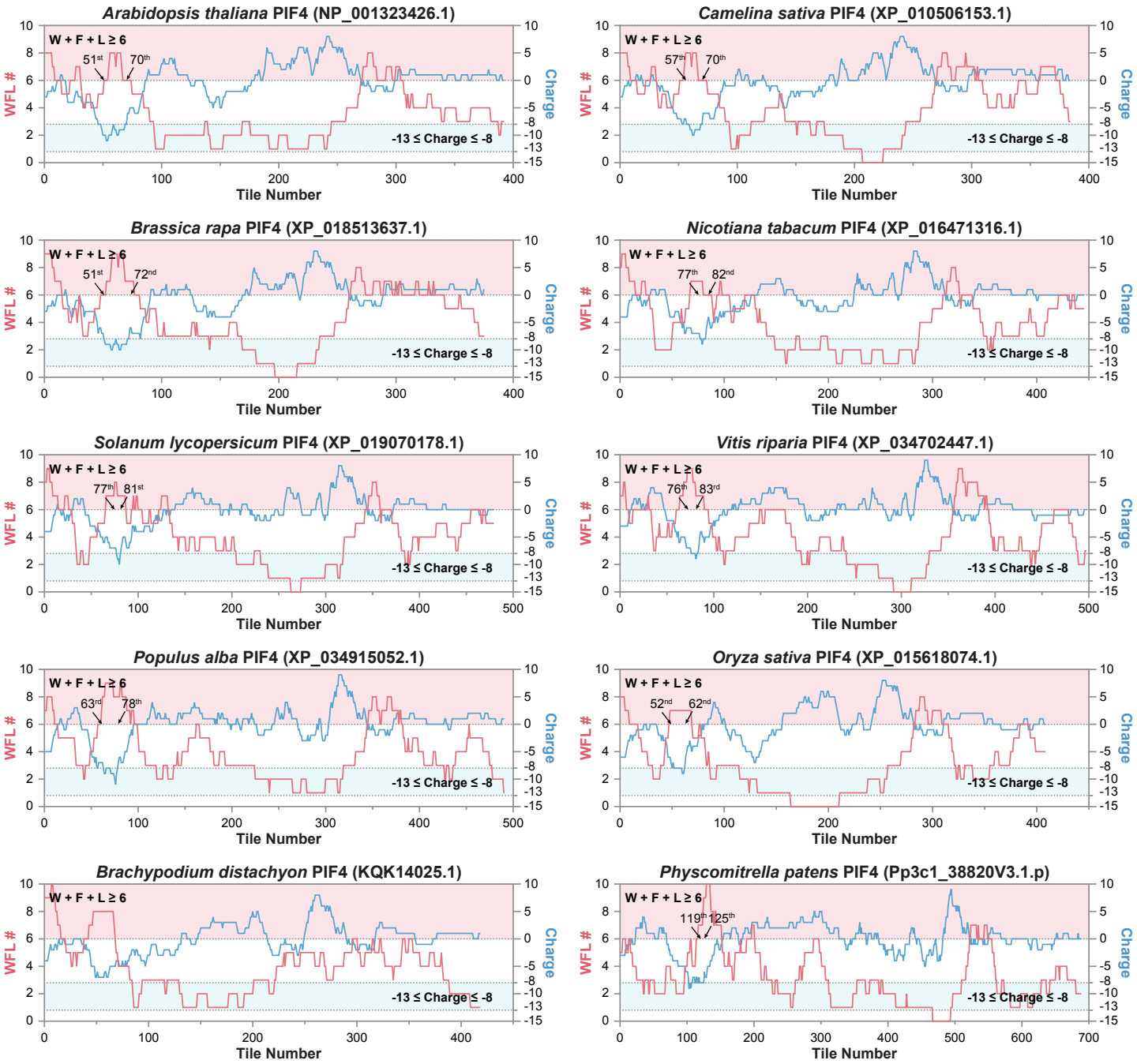

Supplementary Figure 3. A conserved acidic TAD can be identified in PIF4 homologs from different plant species. Schematic representation of a computational analysis dividing PIF4 from various plant species into overlapping 39-amino-acid (a.a.) tiles, spaced by 1 a.a. All tiles were analyzed for hydrophobic (W, F, L) and acidic (D, E) residue content. Regions meeting the criteria of an acidic transactivation domain, as predicted by Kotha and Staller (2023)[70], are shaded red and blue. Criteria include W+F+L ≥ 6 and -13 ≤ Charge ≤ -8.

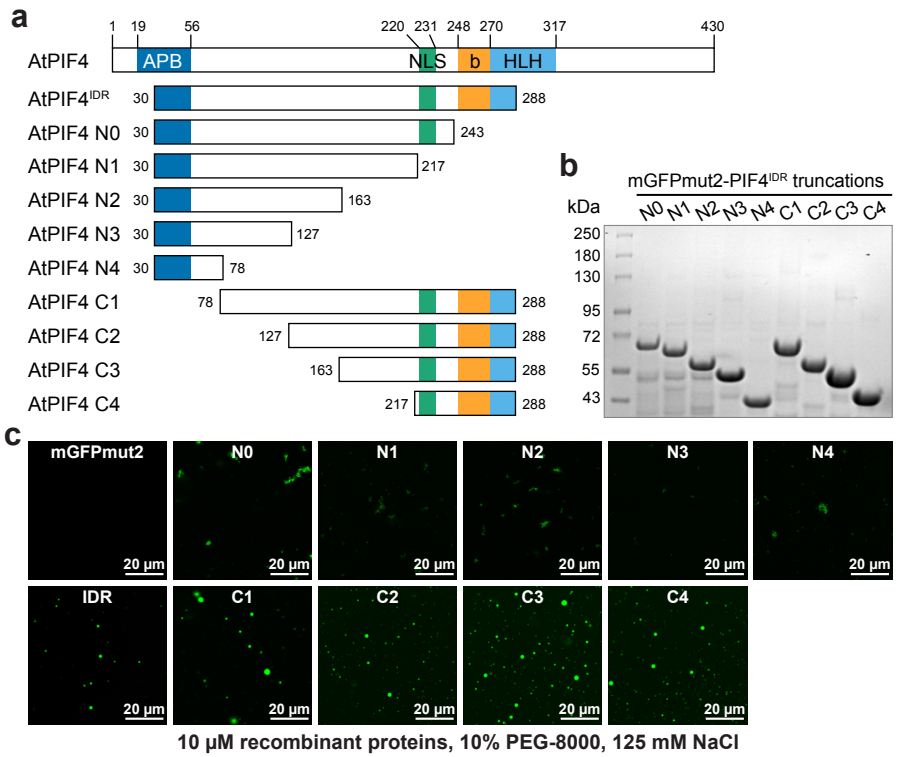

Supplementary Figure 4. Determining the minimal region of PIF4 IDR required for phase separation. a, Schematic representation of truncation constructs derived from the intrinsically disordered region (IDR) of *Arabidopsis thaliana* PIF4 (AtPIF4). Abbreviations: APB, active phyB-binding motif; NLS, nuclear localization signal; bHLH, basic helix-loop-helix domain. Each truncation was fused to mGFPmut2 at the N-terminus to generate recombinant proteins for phase separation analysis. **b**, Coomassie blue staining of purified recombinant proteins used in phase separation assays. **c**, In vitro phase separation assays of mGFPmut2-PIF4^{IDR} truncation proteins. Recombinant proteins (10 μM) were incubated in 10% PEG-8000 with 125 mM NaCl.

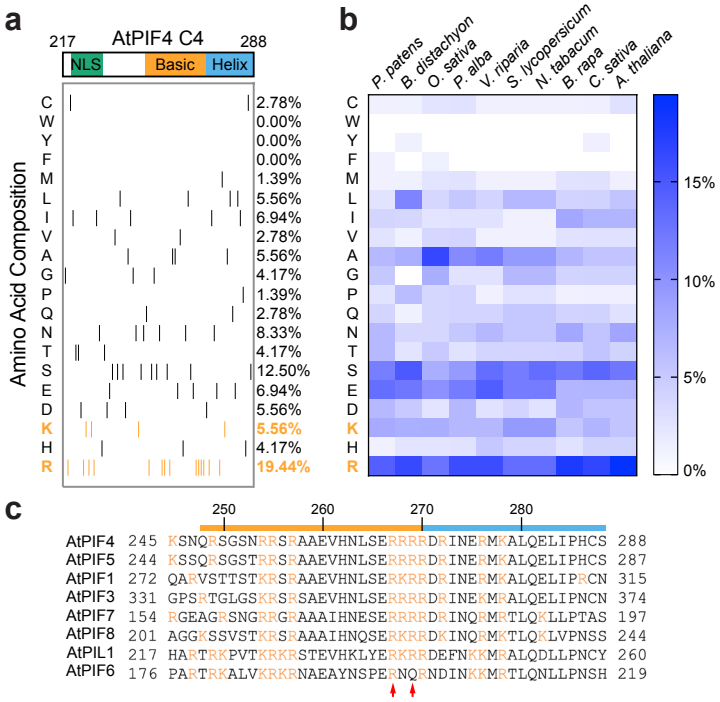

Supplementary Figure 5. Analysis of amino acid composition in PIF4 basic region. a, Amino acid composition in the C4 fragment of AtPIF4. Arginine and lysine residues are highlighted in orange. **b**, Heatmap showing the amino acid composition in the C4 regions of PIF4 homologs. Species include *Arabidopsis thaliana* (NP_001323426.1), *Camelina sativa* (XP_010506153.1), *Brassica rapa* (XP_018513637.1), *Nicotiana tabacum* (XP_016471316.1), *Solanum lycopersicum* (XP_019070178.1), *Vitis riparia* (XP_034702447.1), *Populus alba* (XP_034915052.1), *Oryza sativa* (XP_015618074.1), *Brachypodium distachyon* (KQK14025.1), and *Physcomitrella patens* (Pp3c1_38820V3.1.p). **c**, Sequence alignment of eight Arabidopsis PIF proteins (AtPIL1 is also known as AtPIF2) in the basic region. Red arrows indicate two arginine residues substituted with asparagines in Fig. 8.

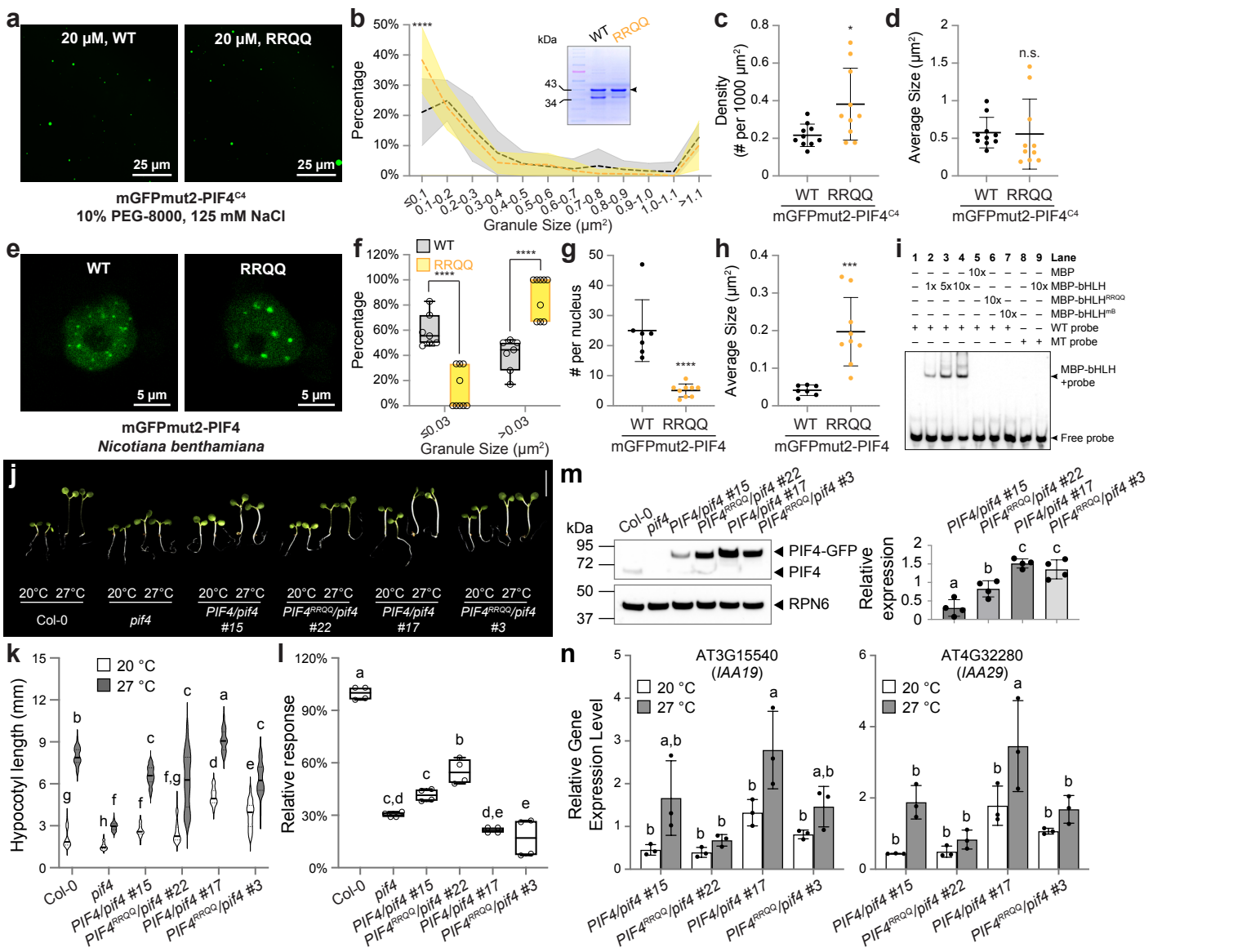

Supplementary Figure 6. The DNA-binding ability of PIF4 is dispensable for its thermomorphogenetic function. a, In vitro phase separation assay of the wild-type and RRQQ mutant versions of mGFPmut2-PIF4^{C4} recombinant proteins. Proteins (20 μM) were incubated in 10% PEG-8000 with 125 mM NaCl. The Coomassie blue staining inside **b** shows protein quality. **b**, Size distribution of mGFPmut2-PIF4^{C4} granules. Wild-type and RRQQ mutant granules were binned into 12 size categories, with the mean percentage for each size bin represented by black (wild-type) or orange (RRQQ) lines, and the standard deviation (SD) shown as shaded areas. Statistical analysis was performed using two-way ANOVA (n = 10; ****, $p < 0.0001$). **c**, Comparison of granule density between wild-type and RRQQ versions of mGFPmut2-PIF4^{C4}. **d**, Average granule sizes of wild-type and RRQQ versions of mGFPmut2-PIF4^{C4}. Statistical significance was assessed using a Student's t-test (n = 10; *, $p < 0.05$; n.s., not significant). **e**, Confocal microscopy images of wild-type and RRQQ versions of mGFPmut2-PIF4 speckles in *N. benthamiana*. **f–h**, Quantitative analysis of mGFPmut2-PIF4 speckles in *N. benthamiana*. **f**, Proportions of smaller (≤ 0.03 μm²) and larger (> 0.03 μm²) speckles. **g**, Number of granules per nucleus. **h**, Average granule size. **i**, EMSA showing MBP-tagged PIF4 bHLH domain binds to G-box of the *IAA19* promoter (WT probe, tatttcatataatttCACGTGgcccaacttgtttct), but not the mutated *IAA19* promoter (MT probe, tatttcatataatttACAACAgcccaacttgtttct). MBP, MBP-bHLH^{RRQQ}, and MBP-bHLH^{mB} all fail to bind to the WT probe. **j**, Representative images of 4-day-old seedlings grown under continuous red light (Rc, 50 μmol m^{-2} s^{-1}) at 20 °C and 27 °C. Genotypes include wild-type (Col-0), *pif4-2* (*pif4*), two lines expressing *PIF4pro::PIF4-mGFPmut2-^{6}His* in the *pif4-2* background (*PIF4/pif4* #15 & #17), and two lines expressing *PIF4pro::PIF4^{RRQQ}-mGFPmut2-^{6}His* in the *pif4-2* background (*PIF4^{RRQQ}/pif4* #22 & #3). **k**, Hypocotyl length measurements of seedlings shown in **j**. White and gray violin plots represent data from 20 °C and 27 °C, respectively. Solid lines denote the median, and dotted lines indicate the first and third quartiles. Different letters indicate statistically significant differences in absolute hypocotyl lengths (two-way ANOVA, n ≥ 65, $p < 0.05$). **l**, Relative thermal response of hypocotyl elongation among the genotypes in **j**. Box plots show the median (center line), first and third quartiles (box limits), and whiskers (minimum and maximum values). Relative response is calculated as the ratio of hypocotyl elongation at 27 °C to 20 °C, normalized to Col-0 (set to 100%). Different letters indicate significant differences between genotypes (one-way ANOVA, n = 3, $p < 0.001$). **m**, Immunoblot analysis of PIF4 protein levels in seedlings in **j**. Seedlings were grown at 20 °C and then transferred to 27 °C for 6 hours under Rc. RPN6 was used as a loading control, and relative PIF4 levels were quantified from four biological replicates. Statistical differences were determined by one-way ANOVA (n = 4, $p < 0.05$). **n**, RT-qPCR analysis of thermo-induced, growth-promoting gene expression levels in the seedlings shown in **j**. Seedlings were grown at 20 °C and then transferred to 27 °C or maintained at 20 °C for 6 hours under Rc. Data was shown from three biological replicates. Different letters denote significant statistical differences (one-way ANOVA, n = 3, $p < 0.05$).

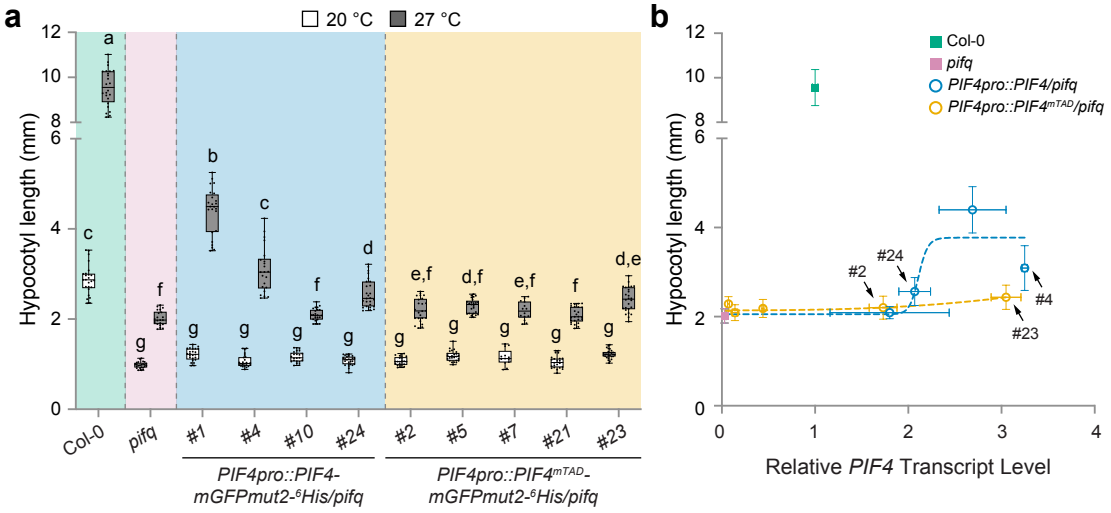

Supplementary Figure 7. Characterizations of *PIF4* transgenic lines in the *pifq* mutant background. a, Hypocotyl length measurements of seedlings. Wild-type (Col-0), *pifq* (*pif1 pif3 pif4 pif5* quadruple) mutant, and transgenic lines expressing *PIF4-mGFPmut2-6His* or *PIF4mTAD-mGFPmut2-6His* driven by the *PIF4* native promoter in the *pifq* mutant background were grown for 4 days in Rc (50 μmol m^{-2} s^{-1}). The white and grey boxes represent hypocotyl length at 20 °C and 27 °C, respectively. The elements of box plots are as follows: center line, median; box limits, first and third quartiles; whiskers, minimum and maximum values; points, all data points. Different letters denote significant statistical differences between the absolute hypocotyl length of each line (two-way ANOVA, n ≥ 13, $p < 0.05$). **b**, Relationship between *PIF4* transcript level and hypocotyl length at warm temperatures. The hypocotyl length of each genotype grown at 27 °C in **a** was plotted against the relative *PIF4* transcript level measured in the same condition (that in Col-0 was set to 1). Nonlinear regression (sigmoidal, 4PL) was performed separately for *PIF4-mGFPmut2-6His/pifq* (blue) and *PIF4mTAD-mGFPmut2-6His/pifq* lines (yellow).